19. DeConinck, F. *Geoderma* **24,** 101–128 (1980).
20. van Breemen, N., Driscoll, C. T. & Mulder, J. *Nature* **307,** 599–604 (1984).
21. Cronan, C. S. & Goldstein, R. A. in *Acidic Precipitation Vol. 1: Case Studies* (eds Adriano, D. C. & Havas, M.) 113–135 (Springer, 1989).
22. Rustad, L. E. & Cronan, C. S. *Biogeochemistry* **29,** 107–129 (1995).
23. Mulder, J., Pijpers, M. & Christophersen, N. *Wat. Resour. Res.* **27,** 2919–2928 (1991).
24. Rustad, L. E. thesis, Univ. Maine, (1988).
25. Cronan, C. S. *Tree Physiol.* **8,** 227–237 (1991).
26. Federer, C. A. *BROOK90 Version* 3.0 (Freeware Computer Program & Documentation, US Forest Service, Durham, NH, 1994).
27. Miller, E. K., Blum, J. D. & Friedland, A. J. *Nature* **362,** 438–441 (1993).
28. Hedin, L. O. *et al. Nature* **367,** 351–354 (1994).

ACKNOWLEDGEMENTS. Archived soil samples were supplied by the Hubbard Brook Ecosystem Study; the Hubbard Brook Experimental Forest is operated by the Northeastern Forest Experiment Station, USDA Forest Service. We thank T. G. Siccama and J. R. Gosz for collection of the archived samples, and D. S. Ross and T. G. Huntington for their reviews of the manuscript. This Letter has not received USDA Forest Service peer review and should not be construed to represent the policies of this agency. This work was supported by USDA Forest Service Global Change Research Program.

Simulation of abrupt climate change induced by freshwater input to the North Atlantic Ocean

Syukuro Manabe & Ronald J. Stouffer

Geophysical Fluid Dynamics Laboratory/NOAA, Princeton University, Princeton, New Jersey 08542, USA

TEMPERATURE records from Greenland ice cores[1,2] suggest that large and abrupt changes of North Atlantic climate occurred frequently during both glacial and postglacial periods; one example is the Younger Dryas cold event. Broecker[3] speculated that these changes result from rapid changes in the thermohaline circulation of the Atlantic Ocean, which were caused by the release of large amounts of melt water from continental ice sheets. Here we describe an attempt to explore this intriguing phenomenon using a coupled ocean–atmosphere model. In response to a massive surface flux of fresh water to the northern North Atlantic of the model, the thermohaline circulation weakens abruptly, intensifies and weakens again, followed by a gradual recovery, generating episodes that resemble the abrupt changes of the ocean–atmosphere system recorded in ice and deep-sea cores[4]. The associated change of surface air temperature is particularly large in the northern North Atlantic Ocean and its neighbourhood, but is relatively small in the rest of the world.

The coupled model[5,6] consists of general circulation models (GCMs) of the atmosphere and oceans and a simple model of land surface that includes the budgets of heat and water. It is a global model with realistic geography. The atmospheric GCM includes the seasonal variation of insolation and predicted cloud cover. It has nine vertical finite-difference levels. The horizontal distributions of predicted variables are represented by spherical harmonics (15 associated Legendre functions for each of 15 Fourier components) and by corresponding grid points. The oceanic GCM uses a finite-difference technique with a regular grid system which has horizontal spacing of 4.5° latitude × 3.75° longitude and 12 vertical levels.

The control experiment is a 1,000-year time integration of the coupled model[7] described above. The initial conditions for the control experiment have realistic seasonal and geographical distributions of surface temperature, surface salinity and sea ice, with which both the atmospheric and oceanic model states are nearly in equilibrium. When the time integration of the model starts from this initial condition, the model climate drifts towards its own equilibrium state which differs from the realistic initial condition described above. To reduce this drift, the fluxes of heat and water obtained from the atmospheric component of the coupled model are modified by given amounts before they are imposed at the oceanic surface. Because the adjustments are determined before the time integration of the coupled model, and are not correlated to the transient surface anomalies of temperature and salinity which can develop during the integration, they are unlikely to either systematically amplify or damp the anomalies. The adjustments do not eliminate the shortcomings of the model dynamics which could distort the simulated transients[8]. But the adjustments do prevent the rapid drift of the model state from the realistic initial condition, which could seriously distort the results of a numerical experiment. The identical adjustments are also applied to the freshwater (FW) experiment described below.

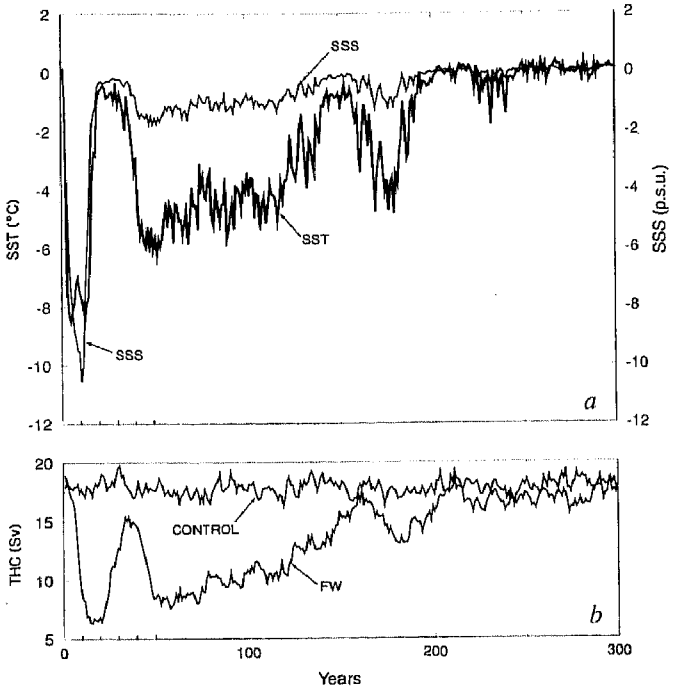

FIG. 1 *a*, Time series of the deviations of sea surface temperature (SST) and sea surface salinity (SSS; p.s.u., practical salinity units) from their initial values (that is, 7 °C and 35 p.s.u., respectively) at a grid point in the Denmark Strait (60.75° N, 37.50° W) obtained from the FW experiment. *b*, Temporal variations of the rate of THC in the North Atlantic obtained from the control and FW integrations. Here, the rate of THC is defined as the maximum value of the stream function of meridional circulation in the North Atlantic (Fig. 4).

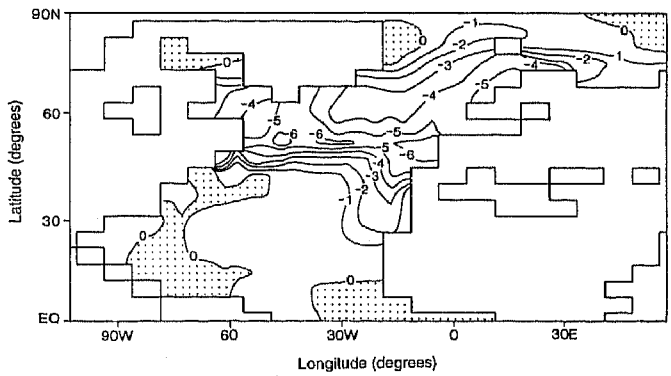

FIG. 2 Horizontal distribution of SSS anomalies (in units of p.s.u.) averaged over the 10-year period from year 11 to year 20 of the FW experiment. The areas of positive anomalies are shaded. Here, the anomaly represents the difference between the 10-year mean state of the FW integration and the 100-year (years 501–600) mean state of the control integration.

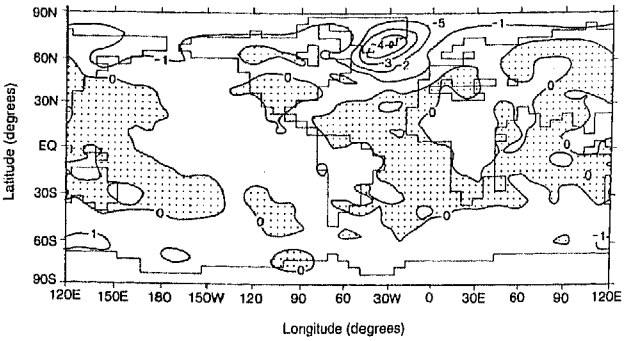

FIG. 3 Horizontal distribution of surface air temperature anomaly (°C) averaged over the 10-year period from year 51 to year 60 of the FW experiment. The areas of positive anomalies are shaded. Here, the anomaly represents the difference between the 10-year mean state of the FW integration and the 100-year (years 501–600) mean state of the control integration.

In the FW experiment conducted here, a surface freshwater flux of 1 Sv (10^6 m^3 s^{-1}) is released uniformly over the latitude belt between ~50 and 70° in the North Atlantic Ocean during the first 10-yr period. Although the freshwater flux is turned off at the end of the tenth year, the time integration is performed over a period of 300 years. (Fairbanks[9] estimated that the rate of the pre-Younger Dryas discharge of melt water into the entire world oceans peaked at 0.44 Sv, which is smaller than the rate of 1 Sv used here. However, the total amount of discharge is much larger than that imposed in the present experiment.) The initial condition for the FW experiment is the state of the coupled ocean–atmosphere model at year 501 of the 1,000-year control integration. The change of the model state induced by the freshwater flux is examined by comparing the FW and control integrations. We note that the melt water is applied to the simulated state of the current interglacial rather than the last glacial period. It is therefore desirable to reassess the response of the thermohaline circulation (THC) in a glacial environment when the glacial states of oceans and the atmosphere have been successfully simulated and the rates of freshwater input into the North Atlantic are better known.

Because of the infusion of fresh water described above, sea surface salinity (SSS) in the Denmark Strait is reduced abruptly during the decade of the water infusion, followed by a rapid recovery as indicated in Fig. 1*a*. By the second decade, the region of large negative SSS anomalies extends to the west of the north African coast and Arctic Ocean (Fig. 2). The reduction of surface salinity during the first decade of the experiment is accompanied by a very rapid lowering of sea surface temperature (SST) centred around the Denmark Strait by as much as 8 °C followed by an almost abrupt warming and cooling (Fig. 1). By the sixth decade, the region of negative SST and surface air temperature anomalies extends from 40° N in the Atlantic to most of Greenland, Scandinavia and the west European coast (Fig. 3). During the next few hundred years, both SST and SSS increase and recover their normal values, with substantial fluctuations around years 120 and 200 (Fig. 1).

The sudden drop of SST during the first decade of the FW experiment results partly from the reduction of convective activity which mixes the cold surface water with the warmer subsurface water of the ocean. The SST drop is also attributable to the rapid weakening of the thermohaline circulation (Fig. 1*b*), which advects warm surface water towards the northern North Atlan-

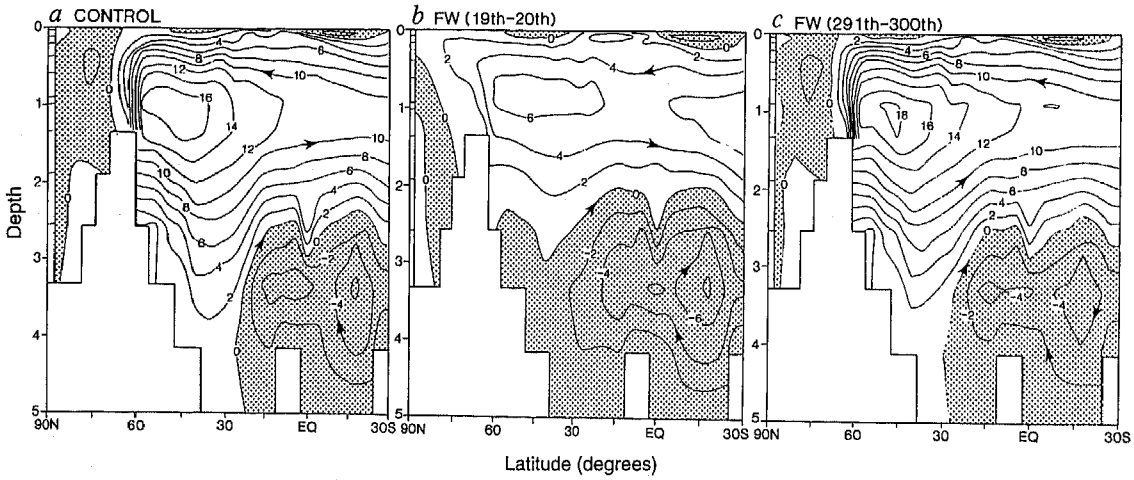

FIG. 4 Latitude–depth distribution of the stream function which represents the meridional overturning in the North Atlantic in units of sverdrups (10^6 m^3 s^{-1}), averaged over: *a*, years 501–600 of the control experiment; *b*, years 19 and 20 and *c*, years 291–300 of the FW experiment. (Depth is given in kilometres; areas of clockwise circulation are shaded.) During the few initial decades, the THC in the North Atlantic markedly weakens and becomes shallower (compare *a* and *b*), allowing stronger deep inflow of Antarctic bottom water. The initial capping of the Atlantic Ocean by the low-density, fresh surface water chokes off the heat exchange between the atmosphere and ocean and raises the temperature of subsurface water, rapidly weakening the THC during the first decade of the experiment. At the end of the second decade, the THC extends poleward of 65° N in the near-surface layer (*b*). The associated extension of the northward advection of warm surface water is responsible for the rapid increase of SST and SSS in the Greenland Sea during the second decade (Fig. 1*a*). The northward extension of warm advection disappears by year 40 of the experiment, causing the reduction of SST and SSS during the fourth decade (Fig. 1*a*). It appears that the northward extension (into the Norwegian/Greenland seas) occurs because the density of surface water is too low to sink at normal latitudes (that is, around 60° N). The gradual recovery and eventual restoration (*c*) of the overturning intensity, which follows the rapid initial fluctuation, is attributable partly to the vertical subsurface water column of relatively high density which is restored in the sinking region of the THC by ~70 years of the experiment. The increase of the water column density is due not only to the horizontal spreading and disappearance of the very fresh surface water but also to the reduced supply of warm water with relatively low density from the south into the sinking region of the THC. The gradual reintensification of the THC is also attributable to the reduction of subsurface water density in low latitudes which is due to the weakened upwelling of dense water associated with the large initial weakening of the THC. The increase in the meridional gradient of density due to the density changes of opposite sign in the sinking and rising regions of the THC results in the increase of not only the meridional but also the zonal density gradient[20] in the upper layer of the ocean, intensifying the meridional circulation and causing the gradual recovery in the intensity of the THC.

tic. The large initial weakening and reintensification of the THC appear to be induced by the massive, initial infusion of fresh, low density water and its abrupt termination, respectively. After the initial fluctuation, the THC reintensifies gradually (Fig. 1*b*), increasing both SST and SSS during the next few hundred years. The damped oscillation of the THC, which occurs during the reintensification, resembles the weaker oscillation which Delworth *et al.*[10] found in the control experiment. The structures of the THC at the beginning, shortly after the termination of the freshwater infusion, and at the end of the experiment are illustrated and discussed in Fig. 4. and its legend.

The coupled model produced large and rapid changes in surface air temperature and the rate of deep-water formation reminiscent of those inferred from the palaeoceanographic[4,11] and ice-core records[1,2]. But during the glacial and postglacial periods, one can identify many cold episodes of low ice-core $\delta^{18}O$ which last much longer than the simulated period of low SST in the present FW experiment. Obviously, the cold period could last longer if a meltwater flux of smaller magnitude were applied much longer than 10 years, or a massive armada of icebergs was discharged and melted in the middle of the cold period[12]. Both of these mechanisms, which release the fresh water with low $\delta^{18}O$, could have operated during the cold event of 14,500 ^{14}C-years ago, accounting for the $\delta^{18}O$ minimum in planktonic foraminifera noted by Keigwin and Lehman[13]. On the other hand, the total amount of melt water infused around the beginning of the Younger Dryas event might have been substantially larger than that imposed in the present experiment[9]. If so, the THC could be weakened enough to keep it at a reduced intensity despite the relatively small supply of fresh water during most of the cold Younger Dryas period. It is likely that the rate of meltwater supply during the Younger Dryas was too small to reverse the positive $\delta^{18}O$ anomaly associated with low SST, yielding the planktonic $\delta^{18}O$ maximum noted by Keigwin and Lehman[13].

By use of a coupled ocean–atmosphere model, Manabe and Stouffer[14] obtained two stable equilibria, that is, active and inactive modes of the THC in the Atlantic Ocean. They suggested that the inactive mode resembles the oceanic state of Younger Dryas. However, the palaeoceanographic evidence[15] indicates not only a markedly reduced deep-water formation but also a significant ventilation of the upper ocean layer during the cold period. It is therefore likely that the transient state of weak and shallow THC encountered during the present FW experiment is more consistent with the palaeoceanographic signatures of Younger Dryas than the inactive equilibrium mentioned above. The freshwater-induced transitions among multiple equilibria of a simple coupled model were examined, for example, by Stocker *et al.*[16] and Rahnstorf[21].

The evolutions of the THC and SST, which were recently obtained by Rahmstorf[17] by use of his coupled model with a highly simplified atmosphere and idealized geography, and without the seasonal variation, is quite different from those described in the present study. His simulation shows that, in response to an infusion of fresh water, the THC rapidly weakens but restores its original intensity very quickly, leaving behind an equilibrium state of shallow convection and cold surface water. In the coupled model used here, it is not possible to sustain such shallow convection indefinitely at a given grid point, because it is influenced by the noisy and seasonally varying atmosphere.

The recent study of Manabe and Stouffer[18,19] reveals that, associated with the CO_2-induced warming of the model atmosphere, the poleward transport of water vapour increases, causing marked increases in precipitation, and accordingly, freshwater supply in the high latitudes. The simulated multi-century response of the THC to the doubling of atmospheric CO_2 (refs 18, 19) resembles the response to the freshwater input described here. Thus substantial changes in the intensity and distribution of the THC could also occur in response to future increases of greenhouse gases in the atmosphere. □

Received 30 May; accepted 3 October 1995.

1. Dansgaard, W. *et al. Science* **218,** 1273–1277 (1982).
2. Johnsen, S. J. *et al. Nature* **359,** 311–313 (1992).
3. Broecker, W. S. *Paleoceanography* **5,** 459–467 (1990).
4. Keigwin, L. D. & Jones, G. A. *J. geophys. Res.* **99,** 12397–12410 (1994).
5. Stouffer, R. J., Manabe, S. & Bryan, K. *Nature* **342,** 660–662 (1989).
6. Manabe, S., Stouffer, R. J., Spelman, M. J. & Bryan, K. *J. Clim.* **4,** 785–818 (1991).
7. Stouffer, R. J., Manabe, S. & Vinnikov, K. Ya. *Nature* **367,** 634–636 (1994).
8. Marotzke, J. & Stone, P. *J. phys. Oceanogr.* **25,** 1350–1364 (1995).
9. Fairbanks, R. G. *Nature* **342,** 637–642 (1989).
10. Delworth, T., Manabe, S. & Stouffer, R. J. *J. Clim.* **6,** 1993–2011 (1993).
11. Boyle, E. A. & Rosener, P. *Paleogeogr. Paleoclimatol. Paleoecol.* **89,** 113–124 (1990).
12. Bond, G. *et al. Nature* **365,** 143–147 (1993).
13. Keigwin, L. D. & Lehman, S. *Paleoceanography* **9,** 185–194 (1994).
14. Manabe, S. & Stouffer, R. J. *J. Clim.* **1,** 841–866 (1988).
15. Boyle, E. A. & Keigwin, L. *Nature* **330,** 35–40 (1987).
16. Stocker, T. F., Wright, D. G. & Mysak, L. A. *J. Clim.* **5,** 773–797 (1992).
17. Rahmstorf, S. *Nature* **372,** 82–85 (1994).
18. Manabe, S. & Stouffer, R. J. *Nature* **364,** 215–218 (1993).
19. Manabe, S. & Stouffer, R. J. *Clim.* **7,** 5–23 (1994).
20. Wright, D. G. & Stocker, T. F. *J. phys. Oceanogr.* **21,** 1713–1724 (1991).
21. Rahnstorf, S. *Nature* **378,** 145–149 (1995).

ACKNOWLEDGEMENTS. We thank A. J. Broccoli, T. L. Delworth, S. Griffies, L. D. Keigwin, J. D. Mahlman and J. Miller who offered valuable comments for improving the manuscript.

Plate boundary reorganization at a large-offset, rapidly propagating rift

R. N. Hey*, P. D. Johnson*, F. Martinez*, J. Korenaga†, M. L. Somers‡, Q. J. Huggett‡, T. P. LeBas‡, R. I. Rusby‡ & D. F. Naar§

* Hawaii Institute of Geophysics and Planetology, School of Ocean and Earth Science and Technology, University of Hawaii, Honolulu, Hawaii 96822, USA
† MIT/WHOI Joint Program, Woods Hole Oceanographic Institution, Woods Hole, Massachusetts 02543, USA
‡ Institute of Oceanographic Sciences, Wormley, Godalming GU8 5UB, UK
§ Department of Marine Science, University of South Florida, St Petersburg, Florida 33701, USA

THE existence of rapidly spinning microplates along the southern East Pacific Rise has been documented by geophysical swath-mapping surveys[1–6], and their evolution has been successfully described by an edge-driven kinematic model[7]. But the mechanism by which such microplates originate remains unknown. Proposed mechanisms[1–10] have generally involved rift propagation[11], possibly driven by hotspots or changes in direction of sea-floor spreading. Here we present geophysical data collected over the Earth's fastest spreading centre, the Pacific–Nazca ridge between the Easter and Juan Fernandez microplates (Fig. 1), which reveal a large-offset propagating rift presently reorganizing the plate boundary geometry. A recent episode of rapid 'duelling' propagation of the historically failing spreading centre in this system has created a 120 × 120 km overlap zone between dual active spreading centres, which may be the initial stage of formation of a new microplate.

The dual spreading centres, shown by shallow ridges and acoustically reflective sea floor, overlap between about 28.5°–29.5° S, 113°–112° W (Figs 2, 3). The West ridge has been propagating south[3,12] for ~1.5 Myr, transferring young Pacific lithosphere to the Nazca plate (shown by the rotated fabric extending northeast from the overlap zone). It is the shallowest part of the entire East Pacific Rise, reaching above 2,100 m. It is also the most highly inflated, defined by cross-sectional area above the average 0.5 Myr depth[30], reaching nearly 9 km^2. This propagator has created a shallow V-shaped area bounded by pseudofaults[11] which indicate a steady propagation rate nearly equal to the spreading rate, ~135 km Myr^{-1}. The characteristic parabolic propagator tip results from the acceleration from no spreading to the full rate[13,14]. Spreading along most of the West ridge